Velocity Dispersion Curves of Guided Waves Propagating in a Free Gradient Elastic Plate: Application to Cortical Bone

Maria G. Vavva

Dept. of Material Science and Engineering, GR 451 10 Ioannina, Greece, and Unit of Medical Technology and Intelligent Information Systems, Dept. of Computer Science, University of Ioannina, GR 451 10 Ioannina, Greece.

Vasilios C. Protopappas

Unit of Medical Technology and Intelligent Information Systems, Dept. of Computer Science, University of Ioannina, GR 451 10 Ioannina, Greece.

Leonidas N. Gergidis

Dept. of Material Science and Engineering, GR 451 10 Ioannina, Greece.

Antonios Charalambopoulos

Dept. of Material Science and Engineering, GR 451 10 Ioannina, Greece.

Dimitrios I. Fotiadis[a)]

Unit of Medical Technology and Intelligent Information Systems, Dept. of Computer Science, University of Ioannina, GR 451 10 Ioannina, Greece

Demos Polyzos

Dept. of Mechanical Engineering and Aeronautics, University of Patras, GR 26 500 Patras, Greece.

running title: Guided waves in gradient elastic bone plates

[a)]E-mail: fotiadis@cs.uoi.gr

ABSTRACT

Ultrasonic characterization of bone has been based on the classical linear elastic theory. However, linear elasticity cannot adequately describe the mechanical behavior of materials with microstructure in which the stress state has to be defined in a non-local manner. In this study, we adopt the simplest form of gradient theory (Mindlin FormII) to theoretically determine the velocity dispersion curves of guided modes propagating in isotropic bone-mimicking plates. Two additional terms are included in the constitutive equations representing the characteristic length in bone: (a) the gradient coefficient g, introduced in the strain energy and (b) the micro-inertia term h, in the kinetic energy. The plate was assumed free of stresses and of double stresses. Two cases were studied for the characteristic length: $h = 10^{-4}$ and $h = 10^{-5}$ m, i.e., at the order of the osteons size. For each case, three subcases for g were assumed, namely $g > h$, $g < h$ and $g = h$. The velocity dispersion curves of guided waves were numerically obtained and compared with the Lamb modes. The results indicate that when the elastic constants are not equal, microstructure affects mode dispersion by inducing both material and geometrical dispersion. In conclusion, gradient elasticity can provide supplementary information to better understand guided waves in bones.

PACS numbers: 43.80.Ev, 43.80.Jz, 43.20.Bi

I. INTRODUCTION

In the quite rich literature of quantitative ultrasound assessment of human bones, some new techniques exploiting guided waves in long bones seem very promising in the early diagnosis of osteoporosis (Bossy *et al.*, 2002; Bossy *et al.*, 2004; Camus *et al.*, 2000; Moilanen, 2008; Nicholson *et al.*, 2002; Njeh *et al.* 1999; Wear, 2007) and the evaluation of fracture healing (Dodd *et al*., 2007; Protoppapas *et al*., 2005). As it is indicated by the name, guided waves are disturbances propagating along the body of a structure. Guided waves are particularly attractive for characterization of bone status because they propagate throughout the cortical thickness and are thus sensitive to both mechanical and geometrical properties. Since they interact continuously with the boundaries of the bone, they propagate in different modes with velocities, which depend on the frequency. Although this multimodal and dispersive nature of guided waves makes their handling, control and measurement much more difficult and complicated than bulk waves, guided ultrasound provides more Non-Destructive Testing parameters than that utilized in the traditional through or axial transmission ultrasonic techniques (Chimenti, 1997). Thus, it is apparent that understanding of how ultrasonic guided waves propagate through a bone is of paramount importance for the qualitative and quantitative inspection process.

Modelling of guided ultrasound in long human bones is an extremely difficult task due to the very complex microstructure of bones. In all the works dealing with guided waves in bones and appearing so far in the literature, the bone is mimicked as a linear elastic and homogenized medium. However, if we consider human bone as a linear elastic material with microstructure, its dynamic mechanical behaviour cannot be described adequately by the classical theory of linear elasticity, because this theory is associated with concepts of homogeneity and locality of stresses. When the material exhibits a non homogeneous behaviour and its dimensions are comparable to the length scale of the microstructure, microstructural effects become important and the state of stress has to be defined in a non-local manner. These microstructural effects can be successfully modelled in a macroscopic framework by employing enhanced elastic theories such as the couple stresses theory proposed by Cosserat brothers (Cosserat and Cosserat, 1909) and generalized later by Eringen as the micropolar elastic theory (Eringen, 1966), the general higher order gradient elastic theory proposed by Mindlin (Mindlin, 1964) and the non-local theory of elasticity of Eringen (Eringen, 1992). For a literature review on the subject of these theories one can consult the review articles (Eringen, 1992; Tiersten and Bleustein, 1974; Exadaktylos and Vardoulakis, 2001), the literature review in the recent paper (Tsepoura *et al.*, 2002) and the book (Vardoulakis and Sulem, 1995).

According to couple stresses theories, as proposed by (Cosserat brothers, 1909; Eringen, 1966) the deformation of the medium is described not only by the displacement vector but also by an independent rotation vector. Displacements and rotations are associated to stresses and couples stresses through constitutive relations, which contrary to the classical theory of elasticity define non-symmetric stress and couple stress tensors. Both Cosserat and micropolar elastic theories have been successfully exploited to explain microstructural size effects in bones (Fatemi *et al.*, 2002; Hsia *et al.*, 2006; Lakes, 1981; Park and Lakes 1986; Yang and Lakes, 1981; Yang and Lakes, 1982; Yoon and Katz, 1983). Due to the rotations, couple stresses theories are able to capture wave dispersion phenomena, which are not observed in the classical theory of elasticity. In the context of wave propagation in couple stresses continuum many papers have appeared the last twenty years in the literature. Some representative are (Chen *et al.*, 2003; Suiker *et al.*, 2001) dealing with wave dispersion in free spaces, (Tomar and Gogna, 1995) solving wave reflection problems in flat interfaces, (Kumar and Partap, 2006; Ottosen *et al.*, 2000) investigating Rayleigh waves in micropolar half spaces and (Kulesh *et al.*, 2007; Midya, 2004) treating propagation of dispersive waves in waveguides. However, no previous work has been reported to investigate guided wave propagation in bones in the context of higher order gradient theories of elasticity.

Higher order gradient theories can be considered as generalizations of linear theory of elasticity, utilizing the displacement vector to describe the deformation of the continuum and introducing in both potential and kinetic energy higher order terms associated with internal length scale parameters which correlate microstructural effects with the macrostructural behaviour of the considered material. In the regime of isotropic linear elastic behaviour, the most general and comprehensive gradient elastic theory is the one due to (Mindlin, 1964; Mindlin, 1965). However, in order to balance the dimensions of strains and higher order gradients of strains as well as to correlate the micro-strains with macro-strains, Mindlin utilized eighteen new constants rendering, thus, his initial general theory very complicated from a physical and mathematical point of view. In the sequel, considering long wave-lengths and the same deformation for macro and micro structure Mindlin proposed three new simplified versions of his theory, known as Form I, II and III, where beyond the two Lamé constants other five ones are introduced instead of sixteen employed in his initial model. In Form-I, the strain energy density function is assumed to be a quadratic form of the classical strains and the second gradient of displacement; in Form-II the second displacement gradient is replaced by the gradient of strains and in Form-III the strain energy function is written in terms of the strain, the gradient of rotation, and the fully symmetric part of the gradient of strain. The most important difference among the aforementioned three simplified versions of the general Mindlin's theory is the fact that the Form-II leads to a total stress tensor, which is symmetric as in the case of classical elasticity. This symmetry avoids the problems introduced by the non-symmetric stress tensors in Cosserat and couple stress theories. Ru and Aifantis (Ru and Aifantis, 1993) and Altan, *et al.* (Altan, *et al.*, 1996) proposed a very simple static and dynamic, respectively, gradient elastic model requiring only one new gradient elastic constant plus the standard Lamé ones. Although elegant, the problem with Aifantis and co-workers models is first the complete lack of a variational formulation considering thus boundary conditions which are not compatible with the corresponding correct ones provided by Mindlin and second the fact that they ignore of the contribution of the inertia of the microstructure to the dynamic behaviour of the gradient elastic material. Both drawbacks were corrected later by (Georgiadis *et al.*, 2004; Vardoulakis and Georgiadis, 1997) proposing two very simple and elegant gradient elastodynamic theories called gradient elasticity with surface energy and dipolar gradient elastic theory, respectively. The latter, exploited in the present work, can be considered as the simplest possible special case of Mindlin's Form II gradient elastic theory. In the framework of wave propagation in infinite and semi-infinite gradient elastic spaces one can mention the works of (Aggelis *et al.*, 2004; Bennet *et al.*, 2007; Chang *et al.*, 1998; Erofeyev, 2003; Georgiadis and Velgaki, 2003; Georgiadis *et al.*, 2004; Papargyri-Beskou *et al.*, 2008; Sluys *et al.*, 1993; Vardoulakis and Georgiadis, 1997; Yerofeyev and Sheshenina, 2005).

Finally, in the non-local theory of elasticity of Eringen (Eringen, 1992) stresses at any point of the considered continuum are assumed to be a function not only of the strains defined at the point itself but also of the strain states defined at all other points of the elastic body. This consideration leads to an integro-differential stress-strain constitutive relation, which contains integrals defined over the entire region of interest and kernels comprising weighted averages of the contributions of the strains of all points of the elastic body. The integro-differential form of the constitutive equations renders non-local elastic theory complex for practical applications. Some special cases where the integro-differential constitutive equations can be converted to differential ones, although convenient for applications in materials with microstructural effects, they can be covered by the aforementioned micropolar and higher order gradient elastic theories (Artan and Altan, 2002; Chakraborty, 2007).

In the present work the simplified Mindlin's Form II or dipolar gradient elastic theory is exploited for the determination of symmetric and anti-symmetric modes propagating in a two dimensional and free of stresses gradient elastic plate. The material properties of the plate as well as the internal length scale parameters introduced by the considered enhanced elastic theory are compatible with the physical properties of human bones. To the authors' best knowledge, no such theory has been proposed up to now for the simulation of propagating guided waves in long bones. The main advantages of the utilized gradient elastic theory as compared to other couple stresses, micropolar, gradient elastic and non-local elastic theories are its simplicity and the symmetry of all classical and non-classical stress tensors involved. The paper is organized as follows: the next section is devoted to the basics of the aforementioned gradient elastic theory. In the same section the dispersion nature of the waves propagating in an infinitely extended gradient elastic continuum is illustrated. Next, in section III the modes corresponding to guided waves traveling in a free gradient elastic plate are explicitly derived. The presentation of the derived symmetric and antisymmetric modes for a bone mimicked plate is taken place in section IV. A comprehensive discussion on the obtained results is demonstrated in section V. Finally, the main conclusions of the present study are drawn.

II. MINDLIN'S FORM II SIMPLIFIED GRADIENT ELASTIC THEORY AND WAVE DISPERSION

Mindlin in the Form II version of his gradient elastic theory (Mindlin, 1964) considered that the potential energy density $\hat{W}$ is a quadratic form of the strains ε_{ij} and the gradient of strains, $\hat{\kappa}_{ijk}$, i.e.

$$\hat{W} = \frac{1}{2}\lambda\varepsilon_{ii}\varepsilon_{jj} + \mu\varepsilon_{ij}\varepsilon_{ij} + \hat{\alpha}_1\hat{\kappa}_{iik}\hat{\kappa}_{kjj} + \hat{\alpha}_2\hat{\kappa}_{ijj}\hat{\kappa}_{ikk} + \hat{\alpha}_3\hat{\kappa}_{iik}\hat{\kappa}_{jjk} + \hat{\alpha}_4\hat{\kappa}_{ijk}\hat{\kappa}_{ijk} + \hat{\alpha}_5\hat{\kappa}_{ijk}\hat{\kappa}_{kji}, \quad (1)$$

where

$$\varepsilon_{ij} = \frac{1}{2}\left(\partial_i u_j + \partial_j u_i\right),\ \hat{\kappa}_{ijk} = \partial_i \varepsilon_{jk} = \frac{1}{2}\left(\partial_i \partial_j u_k + \partial_i \partial_k u_j\right) = \hat{\kappa}_{ikj}\,, \tag{2}$$

with ∂_i denoting space differentiation, u_i the displacement, λ, μ representing Lamé constants and $\hat{\alpha}_1 \div \hat{\alpha}_5$ being constants with units of m^2 explicitly defined in (Mindlin,1964).

Extending the idea of non-locality to the inertia of the continuum with microstructure, Mindlin proposed for the isotropic case an enhanced expression for the kinetic energy density function $\hat{T}$, which beyond velocities includes the gradients of the velocities, i.e.

$$\hat{T} = \frac{1}{2}\rho \dot{u}_i \dot{u}_i + \frac{1}{6}\rho d^2 \partial_i \dot{u}_j \partial_i \dot{u}_j\,, \tag{3}$$

where ρ is the mass density, over dots indicate differentiation with respect to time t and d^2 is another material constant called velocity gradient coefficient (units of m^2.)

Strains ε_{ij} and gradient of strains $\hat{\kappa}_{ijk}$ are dual in energy with the Cauchy and double stresses, respectively, defined as:

$$\hat{\tau}_{ij} = \frac{\partial \hat{W}}{\partial \varepsilon_{ij}} = \hat{\tau}_{ji}\,, \tag{4}$$

$$\hat{\mu}_{ijk} = \frac{\partial \hat{W}}{\partial \hat{\kappa}_{ijk}} = \hat{\mu}_{ikj}\,, \tag{5}$$

which implies that

$$\hat{\tau}_{pq} = 2\mu \varepsilon_{pq} + \lambda \varepsilon_{ii} \delta_{pq}\,, \tag{6}$$

and

$$\begin{aligned}\hat{\mu}_{pqr} = {} & \frac{1}{2}\hat{\alpha}_1 \left[\hat{\kappa}_{rii}\delta_{pq} + 2\hat{\kappa}_{iip}\delta_{qr} + \hat{\kappa}_{qii}\delta_{rp}\right] + 2\hat{\alpha}_2 \hat{\kappa}_{pii}\delta_{qr} + \hat{\alpha}_3 (\hat{\kappa}_{iir}\delta_{pq} + \hat{\kappa}_{iiq}\delta_{pr}) + \\ & + 2\hat{\alpha}_4 \hat{\kappa}_{pqr} + \hat{\alpha}_5 \left(\hat{\kappa}_{rpq} + \hat{\kappa}_{qrp}\right).\end{aligned} \tag{7}$$

The total stress tensor $\hat{\sigma}_{pq}$ is then defined as

$$\hat{\sigma}_{pq} = \hat{\tau}_{pq} - \partial_r \hat{\mu}_{rpq}\,, \tag{8}$$

which is symmetric, since both Cauchy stresses $\hat{\tau}_{pq}$ and relative stresses $\partial_r \hat{\mu}_{rpq}$ are symmetric according to Eqs (4), (5).

Considering an isotropic continuum with microstructural effects confined by a smooth boundary and taking the variation of strain and kinetic energy, according to the Hamilton's principle, one can obtain the following equation of motion of a continuum with microstructure

$$\partial_j(\hat{\tau}_{jk} - \partial_i \hat{\mu}_{ijk}) + F_k = \rho \ddot{u}_k - \frac{1}{3}\rho d^2 \partial_p \partial_p \ddot{u}_k\,, \tag{9}$$

accompanied by the classical and non-classical boundary conditions, respectively:

$$\hat{p}_k = p_k^{prescribed}\,, \tag{10}$$

$$\hat{R}_k = R_k^{prescribed}\,, \tag{11}$$

where the traction vector $\hat{p}_k$ and the double traction vector $\hat{R}_k$ are defined as

$$\hat{p}_k = n_j \tau_{jk} - n_i n_j D\hat{\mu}_{ijk} - (n_j D_i + n_i D_j)\hat{\mu}_{ijk} + (n_i n_j D_l n_l - D_j n_i)\hat{\mu}_{ijk} + \frac{1}{3}\rho d^2 \partial_n \ddot{u}_n\,, \tag{12}$$

$$\hat{R}_k = n_i n_j \hat{\mu}_{ijk}\,. \tag{13}$$

In terms of displacements, the equation of motion (9) obtains the form

$$(\lambda + 2\mu)(1 - \hat{l}_1^2 \nabla^2)\nabla\nabla \cdot \mathbf{u} - \mu(1 - \hat{l}_2^2 \nabla^2)\nabla \times \nabla \times \mathbf{u} = \rho(\ddot{\mathbf{u}} - h^2 \nabla^2 \ddot{\mathbf{u}})\,, \tag{14}$$

where $\mathbf{u}$ stands for displacement vector and

$$\hat{l}_1^2 = 2(\hat{a}_1 + \hat{a}_2 + \hat{a}_3 + \hat{a}_4 + \hat{a}_5)/(\lambda + 2\mu),$$

$$\hat{l}_2^2 = (\hat{a}_3 + 2\hat{a}_4 + \hat{a}_5)/2\mu, \tag{15}$$

$$h^2 = d^2/3.$$

Positive definiteness of $\hat{W}$ (for reasons of uniqueness and stability) requires that (Mindlin, 1964) $\mu > 0,\ \lambda + 2\mu > 0,\ \hat{l}_i^2 > 0$ and $h^2 > 0$.

In the simplest possible case where the potential energy density $\hat{W}$ is defined as

$$\hat{W} = \varepsilon_{ij}\tau_{ij} + g^2\partial_i\varepsilon_{jk}\partial_i\tau_{jk}\,, \tag{16}$$

the constants $\hat{\alpha}_1 \div \hat{\alpha}_5$ become $\hat{\alpha}_1 = \hat{\alpha}_3 = \hat{\alpha}_5 = 0$, $\hat{\alpha}_2 = \lambda g^2/2$, $\hat{\alpha}_4 = \mu g^2$ and the constants $\hat{l}_1^2, \hat{l}_2^2$ in (14), $\hat{l}_1^2 \equiv \hat{l}_2^2 = g^2$. Under the above simplifications, the stresses in Eqs. (6), (7) and (8) become

$$\tau_{ij} = 2\mu\varepsilon_{ij} + \lambda\varepsilon_{ii}\delta_{ij}\,, \tag{17}$$

$$\mu_{ijk} = g^2\partial_i\tau_{jk}\,, \tag{18}$$

$$\sigma_{ij} = \tau_{ij} - g^2\nabla^2\tau_{ij}\,, \tag{19}$$

and the equation of motion i.e., Eq.(14), through the well known identity $\nabla^2 = \nabla\nabla\cdot - \nabla\times\nabla\times$ obtains the simple form:

$$(1-g^2\nabla^2)\left[\mu\nabla^2\mathbf{u} + (\lambda+\mu)\nabla\nabla\cdot\mathbf{u}\right] = \rho(\ddot{\mathbf{u}} - h^2\nabla^2\ddot{\mathbf{u}}), \tag{20}$$

where $g^2\nabla^2\left[\mu\nabla^2\mathbf{u} + (\lambda+\mu)\nabla\nabla\cdot\mathbf{u}\right]$ and $\rho h^2\nabla^2\ddot{\mathbf{u}}$ are the micro-structural and the micro-inertia terms, respectively and the operator ∇^2 is the Laplacian. Taking the divergence and the curl of Eq.(20), it is easy to find the equations governing the propagation of dilatations and rotations, i.e.

$$(\lambda+2\mu)(1-g^2\nabla^2)\nabla^2\nabla\cdot\mathbf{u} = \rho(1-g^2\nabla^2)\nabla\cdot\ddot{\mathbf{u}}\,, \tag{21}$$

$$\mu(1-g^2\nabla^2)\nabla^2\nabla\times\mathbf{u} = \rho(1-g^2\nabla^2)\nabla\times\ddot{\mathbf{u}}\,. \tag{22}$$

Considering plane waves of the form

$$\nabla\cdot\mathbf{u} = Ae^{i(K\hat{\mathbf{k}}\cdot\mathbf{r}-\omega t)},$$

$$\nabla\times\mathbf{u} = \mathbf{A}e^{i(K\hat{\mathbf{k}}\cdot\mathbf{r}-\omega t)}, \tag{23}$$

where $A, \mathbf{A}$ represent the amplitudes, $\mathbf{r}$ stands for the position vector, $\hat{\mathbf{k}}$ is the direction of incidence K, ω are the wave number and the frequency of the propagating waves, respectively, and $\mathrm{i}=\sqrt{-1}$. Inserting Eq. (23) into Eqs. (21) and (22) and representing by C_L, C_T the classical phase velocities of longitudinal (L) and shear (T) waves, respectively, we obtain the following dispersion relation:

$$\omega^2 = C_L^2 \frac{K_L^2\left(1+g^2K_L^2\right)}{1+h^2K_L^2},\ C_L^2 = \frac{\lambda+2\mu}{\rho}, \tag{24}$$

for longitudinal waves and the relation:

$$\omega^2 = C_T^2 \frac{K_T^2\left(1+g^2K_T^2\right)}{1+h^2K_T^2},\ C_T^2 = \frac{\mu}{\rho}, \tag{25}$$

for shear waves. Thus, using the Eqs. (24) and (25), we can obtain expressions for the phase velocities V_L and V_T of the longitudinal and shear waves, respectively, of the form:

$$V_{L,T} = \frac{\omega}{K_{L,T}} = C_{L,T}\sqrt{\frac{1+g^2K_{L,T}^2}{1+h^2K_{L,T}^2}}. \tag{26}$$

Equations (25) and (26) reveal that, unlike the classical elastic case characterized by constant velocities of longitudinal and shear waves and hence non-dispersive wave propagation, the gradient elastic case is characterized by phase velocities for longitudinal and shear waves, which are functions of the wave number, indicating wave dispersion. This dispersion is entirely due to the presence of the two microstructural material constants g^2 and h^2. By letting $g=h=0$ in Eq. (22) it becomes obvious that $V_{L,T}$ = $C_{L,T}$, i.e. the classical elastic case with constant wave speeds and hence no dispersion.

Solving Eqs. (24) and (25) for the wave numbers K_L and K_T, respectively, the following relation is obtained:

$$K_{L,T} = \sqrt{\frac{-\left(C_{L,T}^2-\omega^2h^2\right)+\sqrt{\left(C_{L,T}^2-\omega^2h^2\right)^2+4\cdot C_{L,T}^2g^2\omega^2}}{2C_{L,T}^2g^2}}. \tag{26}$$

Since in a dispersive medium energy propagates with the group velocity $V_{L,T}^{g}$ instead of phase velocity $V_{L,T}$ (Rose, 1999), we can find from Eq. (26) that:

$$V_{L,T}^{g} = \frac{d\omega}{dK_{L,T}} = \sqrt{\frac{K_{L,T}^{2}h^{2}+1}{K_{L,T}^{4}C_{L,T}^{2}g^{2}+K_{L,T}^{2}C_{L,T}^{2}}} \cdot \frac{2K_{L,T}C_{L,T}^{2}\left(K_{L,T}^{4}g^{2}h^{2}+2K_{L,T}^{2}g^{2}+1\right)}{\left(K_{L,T}^{2}h^{2}+1\right)^{2}}. \qquad (27)$$

Figure 1 provides the dispersion curves governing the group velocity of longitudinal (L) and shear (T) waves propagating in an infinitely extended gradient elastic medium for various combinations of g and h as a function of frequency according to Eq. (27).

As it is apparent, for $h = g$ or $h = g = 0$ there is no dispersion and $V_{L,T}^{g} \equiv C_{L,T}$. For $h > g$ there is dispersion, $V_{L,T}^{g} < C_{L,T}$ and $V_{L,T}^{g}$ decreases as frequency increases. As it is mentioned in (Paparguri-Beskou *et al.*, 2008), this is a physically acceptable case, which is in agreement with results of crystal lattice theories for the two-dimensional space (Suiker *et al*, 2001; Yim and Sohn, 2000) and the two-dimensional half-space (Gazis *et al.*, 1960). The relation $h > g$ was first found to lead to results in agreement with lattice theories during the numerical studies of (Georgiadis *et al.*, 2004) for wave dispersion in the half-plane. This case is also in agreement with experimental results on metals and alloys (Erofeyev, 2003; Kondratev, 1990) For $h < g$ there is dispersion, $V_{L,T}^{g} > C_{L,T}$ and $V_{L,T}^{g}$ increases with increasing ω in agreement with experimental results on granular type of materials, such as marble, sand, concrete, granular composites, bones and cellular materials (Aggelis *et al.*, 2004; Chen and Lakes, 1989; Erofeyev, 2003; Lakes, 1982; Stavropoulou *et al.*, 2003).

III. WAVE PROPAGATION IN A GRADIENT ELASTIC FREE PLATE

Considering a free two-dimensional (2D) plate and a Cartesian co-ordinate system Ox_1x_2 with the axis Ox_1 being the axis of symmetry of the plate. Assuming plane strain conditions the components of the displacement vector can be written as:

$$u_1 = u_1(x_1, x_2, t),$$

$$u_2 = u_2(x_1, x_2, t), \tag{28}$$

$$u_3 = 0.$$

Solution to the equation of motion i.e, Eq. (20) is given using the method of potentials. The displacement vector field is decomposed according to Helmhotz decomposition as a gradient of a scalar and the curl of the zero divergence vector, i.e.:

$$\mathbf{u} = \nabla\varphi + \nabla\times\mathbf{A}, \qquad \nabla\cdot\mathbf{A} = 0. \tag{29}$$

Substituting Eq. (29) into the equation of motion derived from the gradient elastic theory, i.e. Eq. (20), the following two partial differential equations are obtained

$$(1 - g^2\nabla^2)\nabla^2\varphi = \frac{1}{C_L^2}\ddot{\varphi}, \tag{30}$$

$$(1 - g^2\nabla^2)\nabla^2\mathbf{A} = \frac{1}{C_T^2}\ddot{\mathbf{A}}. \tag{31}$$

Writing the scalar and vector potentials as $\varphi = \phi(x_1, x_2, t)$ and $\mathbf{A} = (A_1, A_2, A_3): A_1 = A_2 = 0$, $A_3 = \psi(x_1, x_2, t)$, the displacement vector in terms of potentials is expressed as:

$$\mathbf{u} = \hat{x}_1\left(\frac{\partial\phi}{\partial x_1} + \frac{\partial\psi}{\partial x_2}\right) + \hat{x}_2\left(\frac{\partial\phi}{\partial x_2} + \frac{\partial\psi}{\partial x_1}\right). \tag{32}$$

Thus, Eqs. (30) and (31) are expressed as:

$$(1 - g^2\nabla^2)\nabla^2\phi = \frac{1}{C_L^2}(1 - h^2\nabla^2)\ddot{\phi}, \tag{33a}$$

$$(1-g^2\nabla^2)\nabla^2\psi = \frac{1}{C_T^2}(1-h^2\nabla^2)\ddot{\psi} . \tag{33b}$$

Assuming travelling waves in the x_1 direction and standing waves in the x_2 direction of the form

$$\phi = \Phi(x_2)\exp\{i(Kx_1 - \omega t)\} , \tag{34}$$

$$\psi = \Psi(x_2)\exp\{i(Kx_1 - \omega t)\} , \tag{35}$$

where Φ and Ψ are unknown functions. Substituting Eqs. (34), (35) into Eqs. (33a), (33b) respectively, we obtain the following differential equations:

$$-g^2\frac{\partial^4\Phi}{\partial x_2^4} + \left(1+2K^2g^2 - \frac{h^2\omega^2}{C_L^2}\right)\frac{\partial^2\Phi}{\partial x_2^2} + \left(K_L^2 - K^2 - g^2K^4 + h^2K^2K_L^2\right)\Phi = 0 , \tag{36a}$$

$$-g^2\frac{\partial^4\Psi}{\partial x_2^4} + \left(1+2K^2g^2 - \frac{h^2\omega^2}{C_T^2}\right)\frac{\partial^2\Psi}{\partial x_2^2} + \left(K_T^2 - K^2 - g^2K^4 + h^2K^2K_T^2\right)\Psi = 0 . \tag{36b}$$

Note here that K represents the wavenumber of the propagating guided disturbance and $K_L^2 = \omega^2 / C_L^2$ and $K_T^2 = \omega^2 / C_T^2$.

It can be observed that when the volumetric strain gradient coefficient g^2 and the inertia term h^2 becomes zero Eqs. (36a) and (36b) become identical to those obtained in the classical elastic case (Rose, 1999). The solutions of Eqs. (36a) and (36b) admit a representation of the form

$$\Phi(x_2) = Q\sin px_2 + R\cos px_2 + S\exp\{r_p x_2\} + T\exp\{-r_p x_2\} , \tag{37}$$

$$\Psi(x_2) = U\sin qx_2 + V\cos qx_2 + W\exp\{r_s x_2\} + Z\exp\{-r_s x_2\} , \tag{38}$$

where

$$p,q = i\frac{\sqrt{1+2K^2g^2 - K_{L,T}^2h^2 - \sqrt{\left(1+2K^2g^2 - K_{L,T}^2h^2\right)^2 + 4g^2\left(K_{L,T}^2 - K^2 - g^2K^4 + h^2K_{L,T}^2K^2\right)}}}{g\sqrt{2}} , \tag{39}$$

$$r_{p,s} = \frac{\sqrt{1+2K^2g^2 - K_{L,T}^2h^2 + \sqrt{\left(1+2K^2g^2 - K_{L,T}^2h^2\right)^2 + 4g^2\left(K_{L,T}^2 - K^2 - g^2K^4 + h^2K_{L,T}^2K^2\right)}}}{g\sqrt{2}} , \tag{40}$$

and the constants $\left(Q, R, S, T, U, V, W, Z\right)$ are unknown amplitudes, which can be determined by satisfying the classical and non-classical boundary conditions of the problem, respectively:

$$\mathbf{P}\,|_{x_2=d/2} = \mathbf{P}\,|_{x_2=-d/2} = 0\,, \tag{41a}$$

$$\mathbf{R}\,|_{x_2=d/2} = \mathbf{R}\,|_{x_2=-d/2} = 0. \tag{41b}$$

Satisfaction of the boundary conditions result in two systems of four equations: the first for the unknowns R, U, S, Z corresponding to the symmetric modes and the second for unknowns Q, T, V, W the antisymmetric modes. The components of the determinant of the two systems are given in Appendix A. Vanishing of each determinant yields the characteristic dispersion equations for the propagation of the symmetric and antisymmetric modes in a gradient elastic plate.

IV. APPLICATION TO CORTICAL BONE PLATES

In this section, a free 2D gradient elastic plate is considered to have mechanical properties typically used for bone, i.e. Young's modulus $E_{bone} = 14$ GPa, Poisson's ratio $\nu_{bone} = 0.37$ and density $\rho_{bone} = 1500$ Kg/m^3. The plate thickness is 4 mm, which is a common cortical value found in several types of human long bones. The resulting classical bulk longitudinal and shear velocities are 4063 m/s and 1846 m/s, respectively (Bossy *et al.*, 2004; Protopappas *et al.*, 2006). Two different cases for the inertia characteristic length h^2 are investigated. In the first case, denoted herein as Case-1, $h = 10^{-4}$ m, whereas in the second, denoted as Case-2, $h = 10^{-5}$ m. In both cases the values of *h* are comparable to bone's microstructure (Harvesian systems, osteons), i.e. from 10 to 500 μm (Rho *et al.*, 1998).

Regarding the value for g, there is strong experimental evidence (Aifantis, 1999; Georgiadis *et al.*, 2004; Exadaktylos and Vardoulakis, 2001; Lakes, 1995; Lam *et al.*, 2003) that it should be also of the same order as the size of the basic building block of microstructure, e.g. the osteons in bones; however, no final conclusion has been drawn in the literature. Therefore, in the present analysis for each of the previous two cases for h , we consider three subcases for g , resulting totally in six different combinations between g and h . In the first two subcases (Case-1a and Case-1b), g is assumed higher and smaller than h, respectively, whereas in the third subcase (Case-1c), the value of g is assumed to be equal to that of h . For Case-2, three subcases are constructed in a similar way as in Case-1. The values for h and g in each subcase are presented in Table I.

In what follows, the symmetric and antisymmetric modes propagating in the bone-mimicking plate with microstructure, in the form of frequency-group velocity (f, c_g) dispersion curves for the different combinations of g and h are presented. The symmetric and antisymmetric modes obtained from the simplified version of Mindlin's Form II gradient elastic theory, are denoted herein as g_S*n* and g_A*n*, respectively, where $n = 0,1,2...$ represents the mode number.

Figures 2(a), (b) and (c) illustrate the group velocity dispersion curves of the symmetric modes for Cases-1a, 1b and 1c, respectively. The group velocity dispersion curves of the Lamb modes for a classical elastic plate with the same geometrical and mechanical properties are also presented in each figure (dashed lines) for comparison purposes. The Lamb modes are denoted as S*n* and A*n*, where $n = 0,1,2...$ In Figs. 2(a)-(b) it can be observed that the bulk shear wave (denoted as g_c_T.) is dispersive, a result that is in fully agreement with the graphs of Figure 1. More specifically, in Fig. 2(a) which represents Case-1a ($g > h$), the velocity of the bulk shear wave derived from the gradient theory for zero frequency is equal to the bulk shear velocity of the medium in classical elasticity (depicted in the figure by a straight dashed line extending across the whole spectrum, denoted as c_T.). As frequency increases, the dispersion curve of the bulk shear wave predicted by the gradient theory significantly deviates from the bulk shear velocity value in the classical case taking higher values. For Case-1b ($g < h$), g_c_T takes lower values than c_T and the deviation starts after 0.4 MHz but is less pronounced than Case-1a. Finally, in Case-1c ($g = h$), the velocity of the bulk shear wave in the gradient elastic case exhibits no dispersion, as expected, i.e. its value remains constant with increasing frequency exactly the same as the bulk shear velocity of bone.

Concerning the guided waves in Fig. 2(a), the dispersion of the modes predicted by the gradient theory is strongly modified from that of the classical elasticity. The velocity of the lowest order g_S0 mode is similar to that of the Lamb S0 mode for very low frequencies (up to 0.13 MHz). However, as frequency increases, the g_S0 mode starts rapidly to diverge from the S0 mode. It is known that S0, as well as, A0 Lamb modes approach asymptotically the Rayleigh velocity (Rose, 1999). As it is shown in Fig. 1(a), the g_S0 mode seems to approach the dispersive values of the bulk shear wave. Given that in classical elasticity the Rayleigh velocity is very close to the bulk shear velocity ($c_R = 0.92c_T$, where c_R is the Rayleigh velocity) (Rose *et al.*, 1999), we can say that the g_S0 mode converges actually to the velocity of Rayleigh wave, which according to (Georgiadis *et al.*, 2004) is also dispersive.

The velocity dispersion of the higher-order modes is considerably different from the Lamb modes, even at low frequencies. More specifically, g_S1 and g_S2 have different cut-off frequencies (0.46 MHz and 0.51 MHz, respectively), their group velocities rapidly increase with frequency and seem to converge to the velocity value of the bulk shear wave in the gradient elasticity (note that in classical elasticity the group velocities of the higher-order Lamb modes converge to the bulk shear velocity of bone). Additional modes, such as g_S3, are expected but they appear at higher frequencies than those computed. Similarly, in Case-1b ($g < h$), the dispersion curves of the guided modes also diverge from the classical Lamb modes (the mode g_S3 can now be seen in this case). Similarly to what occurred for the bulk shear wave, the modes' group velocities take again lower values than those of the classical Lamb waves; nevertheless their deviation is again less pronounced than in Case-1a. In this case, the convergence of the modes to the bulk shear velocity can be better observed.

As opposed to the aforementioned two subcases, in Case-1c ($g = h$), small differences exist in mode dispersion between the two theories of elasticity. The theory predicts that no differences should exist, thus the small deviation observed is due to arithmetic problems.

Figures 3(a), (b) and (c) represent the group velocity dispersion curves of the antisymmetric modes obtained from the gradient elastic plate in Cases-1a, b and c respectively. Similarly to the bulk shear waves and as it is expected (Fig. 1) the bulk longitudinal wave, denoted in the figures as g_c_L, becomes dispersive. The bulk longitudinal velocity, denoted herein as g_$c_{L,}$ for very low frequencies is equal to that of the bulk longitudinal wave propagating in a classical elastic medium (depicted by a straight dashed line and is denoted as c_L). Nevertheless, for higher frequencies in Case-1a, the g_c_L rapidly increases from the bulk longitudinal velocity in the classical case, whereas in Case-1b, it decreases exhibiting a similar behavior to the corresponding bulk shear wave. In Case-1c ($g = h$), as expected, the bulk longitudinal wave in the gradient elastic case is non-dispersive.

Regarding the velocity dispersion of the antisymmetric guided modes, similar conclusions can be drawn to those for the symmetric modes. In particular, in Case-1a (Fig. 3(a)), the group velocities of the g_A0 and g_A1 modes are close to those of the Lamb A0 and A1 modes for very low frequencies, but as the frequency increases they become significantly higher than the Lamb modes. Analogous trends are also observed for the g_A2 and g_A3 modes. These modes converge to the bulk shear values. In Case-1b (Fig. 3(b)), the antisymmetric modes are again affected by the microstructure; the group velocities are lower than those of Lamb modes and the effect is less pronounced than Case-1a. Finally, in the Case-1c (Fig. 3(c)), the velocity dispersion curves are again almost identical to those for the Lamb waves.

Figures 4(a)-(c) and 5(a)-(c) illustrate the group velocity dispersion curves for Case-2, i.e. for $h = 10^{-5}$. Similar trends can be observed for all subcases (Figs. 4(a)-(c) and Figs. 5(a)-(c)), but the observed microstructural effects are much more mitigated than in Figs. 2(a)-(c) and 3(a)-(c).

V. DISCUSSION

In this paper, a study on the propagation of ultrasound in a free plate with microstructural effects was presented. The dipolar gradient elasticity is the enhanced theory exploited for the dynamic behavior of the considered plate. Comparisons with the solutions derived from the Lamb problem in the classical elasticity were also made to investigate the effect of the microstructure on guided wave propagation in 2D plates. Group velocity dispersion curves were obtained for a testing case in which the medium was assumed to have properties similar to those of cortical bone.

As it is mentioned in the introduction, the bone is a material with microstructural effects, the mechanical behavior of which can be successfully modeled by enhanced elastic theories. Although, in the works of (Fatemi *et al*., 2002; Yoon and Katz, 1983) many higher order elastic theories are proposed for the description of the micromechanical effects in bones, only couple stresses theories (mainly Cosserat and micropolar) have been utilized up to now for this purpose. The main reasons for this are: (i) the use of Cosserat-micropolar theories in bending and torsion problems seems to be the most reasonable due to introduction of couple stresses, (ii) the higher order gradient elastic theories of Mindlin as initially proposed were much more complicated than those of couple stresses and (iii) for numerical solutions, the forth order derivatives introduced in the differential operators of the higher order gradient elastic equilibrium equations and equations of motion renders the development of a direct finite element algorithm a difficult task since C(1)-

continuity elements are required. However, during the last decade the simplified versions of Mindlin's general gradient elastic theory (Georgiadis *et al*,. 2004; Ru and Aifantis, 1993; Tsepoura *et al*., 2002; Vardoulakis and Georgiadis, 1997) have gained much attention since: (i) only one microstructural parameter for static problems and two for dynamic ones have to be determined instead of four required in couple stresses theories, (ii) in contrary to Cosserat and micropolar elasticity, all tensors involved in the aforementioned gradient elastic theories are symmetric being thus mathematically simpler and more understandable from a physical point of view and (iii) for fracture mechanics problems (very important for applications in bones) gradient elastic theories lead to more reasonable results than couple stresses ones (Amanatidou and Aravas, 2002; Karlis *et al*., 2007; Karlis *et al*., 2008; Stamoulis and Giannakopoulos, 2008) predicting phenomena associated with cusp-like crack profiles and development of process zone in front of crack tip observed experimentally.

The problem of wave propagation in plates with microstructure has been solved analytically only in the context of the Cosserat theory (Kulesh *et al*., 2007). The same problem is treated here with the aid of the dipolar gradient elastic theory. The values of the inertia internal characteristic length h were assumed to be close to the size of the osteons which correspond to the microstructural level of bone's hierarchical structural organization (Rho *et al.*, 1998). Since the determination of the gradient coefficient g remains an open issue in the literature, we considered six different combinations between g and h. The obtained results make clear that the values of the two length scale parameters g and h play an important role in the velocity trends of the guided modes. In all subcases the values of g were appropriately chosen so as to provide physically acceptable dispersion curves (see Table I). The values: $g = 10^{-3}$ m in Case-1 and $g = 10^{-6}$ m in Case-2 were deliberately ignored here; the former value leads to a rapid increase of the group velocities even from very low frequencies which would be rather undetectable in the plots, whereas the latter would result in almost unnoticeable differences in the velocity variation between the two theories. Thus, it is apparent that reasonable estimations for the relation between the material coefficients and the determination of their values can only be made by comparing experimental measurements with those predicted by the theory. In the analytical study of (Georgiadis *et al*., 2004) dealing with Rayleigh wave dispersion in a gradient elastic half-plane, the value of $g = 4\times10^{-5}$ m is proposed as the best value to describe sufficiently Rayleigh wave dispersion in a geomaterial. However, it is obvious that the value of g varies according to the mechanical properties of the testing material. Therefore, our results should be interpreted in conjunction with measurements from real bones to decide on which is the most suitable combination to provide more realistic dispersion curves.

Figures 2, 3 and 4 reveal that the bulk longitudinal and shear waves propagating in the gradient elastic plate are dispersive, which is in agreement with the propagation of plane waves in an infinitely extended gradient elastic medium addressed by (Papargyri-Beskou *et al*., 2008) and the results depicted in Figure 1. For some combinations of g and h, the deviation of the obtained velocity dispersion of the bulk waves from the constant velocity of the classical elastic ones becomes significant. For instance, in the Case-1a at 1MHz, i.e. for wavelength ≈ 4 mm, the velocity of the bulk longitudinal wave was changed as much as 16% between the classical and the gradient theory of elasticity. This may play an important role when interpreting axial-transmission velocity measurements along the long axis of a bone as it is reported in previous experimental studies of (Njeh *et al*., 1999; Protopappas *et al*., 2005). In the considered plate, for different values of g and h and for frequencies from 0.5 MHz (i.e. for wavelength ≈ 8 mm) to 1.5 MHz (i.e. for wavelength ≈ 2.7 mm), which is the commonly used spectrum in the ultrasonic bone studies (Protopappas *et al*., 2008), the velocity dispersion of the guided waves was significantly modified from that of the Lamb waves. In a previous study (Protopappas *et al*., 2006), by superimposing the theoretical Lamb wave dispersion curves, computed for a bone-mimicking plate, on the time-frequency representation of the signal obtained from ex vivo measurements on an intact tibia, we found that the propagating guided waves could not be sufficiently characterized by the Lamb modes. Therefore, the Lamb wave theory has limited efficiency in predicting wave guidance phenomena in real bones. This was further supported by the findings of two subsequent 3D computational studies (Bossy *et al*, 2004; Protopappas *et al*., 2007) showing that for the same frequency excitation, irregularities in the tubular geometry of the cortex as well as the anisotropy and inhomogeneity of the bone also give rise to major changes in the dispersion of the modes predicted by the classical tube theory. To this end, the results obtained in the present analysis clearly show that the material dispersion induced by the bone's microstructure even in frequencies well below 1 MHz is an additional parameter, which significantly affects the characteristics of wave propagation in bone.

Finally, when the two internal material lengths g and h become zero or equal to each other the presented theory provides velocity dispersion curves being identical to those of the classical elasticity. Nevertheless, in the present study for $g = h$ slight differences between the two theories of elasticity are observed, obviously due to arithmetic errors in the solution of the system of algebraic equations.

VI. CONCLUSIONS

In this work we presented an analytical study on guided wave propagation in 2D bone-mimicking plates with microstructure. For the first time the simple theory of gradient elasticity is proposed to incorporate bone's microstructural effects into the stress analysis. Hence, two additional elastic constants (i.e. the g and h) associated with micro-elastic and micro-inertia effects were considered. In accordance with the findings of a previous study (Papargyri-Beskou *et al.*, 2008), we demonstrated that when the elastic constants have different values, microstructure plays a significant role in the propagation of the bulk longitudinal and shear waves by inducing material and geometrical dispersion. It was also shown that the insertion of the microstructural characteristics into the stress analysis gives rise to major changes in the dispersion of the guided modes predicted by the classical Lamb wave theory. Although previous studies (Georgiadis *et al.*, 2004) report that the microstructural effects are important only at high frequencies, in the present work it was made clear that they can be equally significant at medium frequencies, i.e. 0.7-1 MHz (i.e., for wavelengths from 2.8 mm to 4 mm); which are within the region of interest in ultrasonic bone studies. The effect was dependent on the absolute values of the coefficients and was less pronounced for the smallest value of h (i.e. Cases-2a, 2b). However, reasonable estimations for the relation between the material coefficients and the determination of their values can only be made by comparing experimental measurements with those predicted by the theory. Our findings show that bone's microstructure is an important factor which should be taken into account both in theoretical and computational studies on wave propagation in bones. The gradient theory of elasticity could provide more accurate interpretation of clinical measurements on intact and healing long bones. This study could be regarded as a step towards the ultrasonic evaluation of bone.

VII. APPENDIX A

The components of the determinant for of the two systems which correspond to the symmetric modes

$$
\begin{aligned}
A_{11} &= \left(4\mu p^3 + 2\lambda k^2 p + 2\lambda p^3\right)\sin ph \\
A_{12} &= 4\mu ikq^2 \sin qh \\
A_{13} &= \left(4\mu r_p^3 - 2\lambda k^2 r_p + 2\lambda r_p^3\right)\sin r_p h \\
A_{14} &= -4\mu ikr_s^2 \sin hr_s h \\
A_{21} &= -4\mu ikp^2 \cos ph \\
A_{22} &= 2\mu\left(-q^3 + k^2 q\right)\cos qh \\
A_{23} &= 4\mu ikr_p^2 \cos r_p h \\
A_{24} &= 2\mu\left(r_s^3 + k^2 r_s\right)\cos r_s h \\
A_{31} &= \left(4\mu pik + 4\mu p^3 ikg^2 + 2\lambda p^3 ikg^2 + 2\lambda pik^3 g^2 + 8\mu pik^3 g^2 - \frac{2\rho h^2\omega^2}{3}\right) ikp \sin ph \\
A_{32} &= \left(2\mu q^2 - 2\mu k^2 + 2\mu q^4 g^2 + 4\mu k^2 q^2 g^2 - 2\mu k^4 g^2 - \frac{2\rho h^2\omega^2}{3} q^2\right)\sin qh \qquad \text{(A1)} \\
A_{33} &= \left(-4\mu r_p ik + 4\mu r_p^3 ikg^2 + 2\lambda r_p^3 ikg^2 - 2\lambda r_p ik^3 g^2 - 8\mu ik^3 r_p g^2 + \frac{2\rho h^2\omega^2}{3} ikp\right)\sin hr_p h \\
A_{34} &= \left(-2\mu r_s^2 + 2\mu r_s^4 g^2 - 2\mu k^4 g^2 - 2\mu k^2 - 4\mu k^2 r_s^2 g^2 + \frac{2\rho h^2\omega^2}{3} r_s^2\right)\sin hr_s h \\
A_{41} &= (-4\mu p^2 - 2\lambda p^2 - 2\lambda k^2 - 2\lambda p^4 g^2 - 4\mu p^4 g^2 - 2\lambda k^4 g^2 - 4\lambda k^2 p^2 g^2 \\
&\quad - 8\mu k^2 p^2 g^2 + \frac{2\rho h^2\omega^2}{3} p^2)\cos ph \\
A_{42} &= \left(-4\mu qik - 2\mu q^3 ikg^2 - 6\mu ik^3 qg^2 + \frac{2\rho h^2\omega^2}{3} ikq\right)\cos qh \\
A_{43} &= (4\mu r_p^2 + 2\lambda r_p^2 - 2\lambda k^2 - 2\lambda r_p{}^4 g^2 - 4\mu r_p^4 g^2 - 2\lambda k^4 g^2 + 4\lambda k^2 r_p^2 g^2 \\
&\quad + 8\mu k^2 g^2 r_p^2 - \frac{2\rho h^2\omega^2}{3} r_p^2)\cos hr_p h \\
A_{44} &= \left(-4\mu r_s ik + 2\mu r_s^3 ikg^2 - 6\mu ik^3 r_s g^2 + \frac{2\rho h^2\omega^2}{3} ikr_s\right)\cosh hr_s h
\end{aligned}
$$

and for the anti-symmetric are:

$$B_{11} = \left(-4\mu p^3 - 2\lambda k^2 p - 2\lambda p^3\right)\cos ph$$
$$B_{12} = 4\mu ikq^2 \cos qh$$
$$B_{13} = -4\mu ikr_s^2 \cosh r_s h$$
$$B_{14} = \left(4\mu r_s^3 - 2\lambda k^2 r_p + 2\lambda r_p^3\right)\cosh r_p h$$
$$B_{21} = 4\mu ikp^2 \sin ph$$
$$B_{22} = -2\mu\left(q^3 - k^2 q\right)\sin qh$$
$$B_{23} = -2\mu\left(r_s^3 + k^2 r_s\right)\sinh r_s h$$
$$B_{24} = -4\mu ikr_p^2 \sinh r_p h$$
$$B_{31} = (4\mu pik + 4\mu p^3 ikg^2 + 2\lambda p^3 ikg^2 + 2\lambda ik^3 pg^2 + 8\mu ik^3 pg^2)\cos ph$$
$$B_{32} = (-2\mu q^2 + 2\mu k^2 - 2\mu q^4 g^2 - 4\mu k^2 q^2 g^2 + 2\mu k^4 g^2 + \frac{2\rho h^2\omega^2}{3} q^2)\cos qh$$
$$B_{33} = (2\mu r_s^2 - 2\mu r_s^4 g^2 + 2\mu k^4 g^2 + 2\mu k^2 + 4\mu k^2 r_s^2 g^2 - \frac{2\rho h^2\omega^2}{3} r_s^2)\cosh r_s h \qquad \text{(A2)}$$
$$B_{34} = (4\mu r_p ik - 4\mu ikg^2 r_p^3 - 2\lambda r_p^3 ikg^2 + 2\lambda ik^3 r_p g^2 + 8\mu ik^3 r_p g^2 - \frac{2\rho h^2\omega^2}{3} ikr_p)\cosh r_p h$$
$$B_{41} = (4\mu p^2 + 2\lambda p^2 + 2\lambda k^2 + 2\lambda p^4 g^2 + 4\mu p^4 g^2 + 2\lambda k^4 g^2 +$$
$$4\lambda k^2 p^2 g^2 + 8\mu k^2 p^2 g^2 - \frac{2\rho h^2\omega^2}{3} p^2)\sin ph$$
$$B_{42} = \left(-4\mu ikq - 2\mu ikq^3 g^2 - 6\mu ik^3 qg^2 + \frac{2\rho h^2\omega^2}{3} ikq\right)\sin qh$$
$$B_{43} = \left(4\mu r_s ik - 2\mu r_s^3 g^2 ik + 6\mu ik^3 r_s g^2 - \frac{2\rho h^2\omega^2}{3} ikr_s\right)\sinh r_s h$$
$$B_{44} = (-4\mu r_p^2 - 2\lambda r_p^2 + 2\lambda k^2 + 2r_p^4 g^2 + 4\mu r_p^4 g^2 + 2\lambda k^4 g^2 -$$
$$-4\lambda k^2 r_p^2 g^2 - 8\mu k^2 r_p^2 g^2 + \frac{2\rho h^2\omega^2}{3} r_p^2)\sinh r_p h$$

VIII. ACKOWLEDGEMNENTS

This work is part funded by the General Secreteriat of Research and Development, Hellenic Ministry of the Development (“PENED 2003” 03ED140).

References

Aggelis, D.G., Philippidis, T.P., Tsinopoulos, S.V., and Polyzos, D. **(2004)**. "Wave dispersion in concrete due to microstructure," *CD-ROM Proceedings of the 2004 Int. Conference on Computational & Experimental Engineering & Sciences,* Madeira, Portugal, 26-29 July.

Aifantis, E.C. **(1999)**. "Strain gradient interpretation of size effects," Int. J. Fract. **95**, 299–314.

Altan, B.S., Evensen, H., Aifantis, and E.C. **(1996)**. "Longitudinal vibrations of a beam: a gradient elasticity approach," Mech. Res. Commun. **23**, 35–40.

Amanatidou E., and Aravas N. **(2002)**. "Mixed finite element formulations of strain-gradient elasticity problems," Comp. Meth. Appl. Mech. Eng. **191**, 1723-1751.

Artan, R., and Altan, B. **(2002)**. "Propagation of sv waves in a periodically layered media in nonlocal elasticity," Int. J. Solid. Struct. **39**, 5927–5944.

Bennet, T., Gitman, I.M., Askes, H. **(2007)**. "Elasticity theories with higher order gradients of inertia and stiffness for modelling of wave dispersion in laminates," Int. J. Fract. **148**, 185-193.

Bossy, E., Talmant, M., and Laugier, P. (**2002**). "Effect of cortical thickness on velocity measurements using ultrasonic axial transmission: a 2D simulation study," J. Acoust. Soc. Am. **112**(1), 297-307.

Bossy, E., Talmant, M., and Laugier, P. **(2004)**. "Three-dimensional simulations of ultrasonic axial transmission velocity measurement on cortical bone models," J. Acoust. Soc. Am. **115** (5), 2314–2324.

Camus, E., Talmant, M., Berger, G., and Laugier, P. **(2000)**. "Analysis of the axial transmission technique for the assessment of skeletal status," J. Acoust. Soc. Am. **108** (6), 3058–3065.

Chakraborty, A. **(2007)**. "Wave propagation in anisotropic media with non-local elasticity," Int. J. Sol. Struct. **44**, 5723-5741.

Chang, C.S., Gao, J., and Zhong, X. **(1998)**. "High-gradient modeling for Love wave propagation in geological materials," J. Eng. Mech. **124**(12), 1354-1359.

Chen, C.P., and Lakes, R.S. **(1989)**. "Dynamic wave dispersion and loss properties of conventional and negative Poisson's ratio polymeric cellular materials," Cell. Polym. **8**, 343-369.

Chen, Y., Lee, J.D., and Eskandarian, A. **(2003).** "Examining the physical foundation of continuum theories from the viewpoint of phonon dispersion relation," Int. J. Eng. Science **41**, 61-83.

Chimenti, D. E., **(1997)**. "Guided waves in plates and their use in material characterization," Applied Mechanics Review **50**, 247–284.

Cosserat, E. and Cosserat, F. **(1909)**. *Théorie des Corps Déformables* (Hermann et Fils, Paris).

Dodd, S.P. Cummingham, J.L., Miles, A.W., Gheduzzi, S., and Humphrey, V.F. **(2007)**. "An in vitro study of ultrasound signal loss across simple fractures in cortical bone mimics and bovine cortical bone samples," Bone **40**(3), 656–661.

Eringen, A.C. **(1966)**. "Linear theory of micropolar elasticity," J. Math. Mech. **15**, 909–923.

Eringen, A.C. **(1992)**. "Vistas of Nonlocal Continuum Physics," Intern. J. Eng. Science **30**(10), 1551-1565.

Erofeyev, V.I. **(2003)**. *Wave Processes in Solids with Micro-structure* (World Scientific, Singapore).

Exadaktylos, G.E., and Vardoulakis, I. **(2001)**. "Microstructure in linear elasticity and scale effects: a reconsideration of basic rock mechanics and rock fracture mechanics," Tectonoph. **335**, 81-109.

Gazis, D.C., Herman, R., and Wallis, R.F. **(1960)**. "Surface elastic waves in cubic crystals," Phys. Rev. **119**, 533-544.

Georgiadis, H.G., and Velgaki, E.G. **(2003)**. "High-frequency Rayleigh waves in materials with micro-structure and couple-stress effects," Int. J. Solids Struct. **40**, 2501-2520.

Georgiadis, H.G., Vardoulakis, I., and Velgaki, E.G. **(2004)**. "Dispersive Rayleigh-wave propagation in microstructured solids characterized by dipolar gradient elasticity," J. Elasticity **74**, 17-45.

Hsia, S., Chiu S., and Cheng J. **(2006)**. "Wave propagation at the human muscle-compact bone interface," Theoret. Appl. Mech. **33**(3), 223-243.

Karlis, G. F., Tsinopoulos, S. V., Polyzos, D., and Beskos, D. E. **(2007)**. "Boundary element analysis of mode I and mixed mode (I and II) crack problems of 2-D gradient elasticity," Comp. Meth. Appl. Mech. Eng., **196**, 5092–5103.

Karlis, G. F., Tsinopoulos, S. V., Polyzos, D., and Beskos, D. E. **(2008)**, "2D and 3D Boundary Element Analysis of Mode-I Cracks in Gradient Elasticity," Comp. Model. Eng. Sciences, **26**(3), 189-207.

Kondratev, A.I. **(1990)**. "Precision measurements of the velocity and attenuation of ultrasound in solids," Sov. Phys. Acoust. **36**, 262-265.

Kulesh, M.A., Matveenko, V.P., and Shardakov, I.N. **(2007)**. "Constructing an solution for Lamb waves using Cosserat continuum approach," J. App. Mech. and Techn. Phys. **48**(1), 119-125.

Kumar, R., and Partap, G. **(2006)**. "Rayleigh Lamb waves in micropolar isotropic elastic plate," App. Math. and Mech. **27**(8), 1049-1059.

Lakes, R.S. **(1981)**. "Dynamical study of couple stress effects in human compact bone," J. Biomech. Eng. **104**(1), 6–11.

Lakes, R.S. **(1995)**. "Experimental methods for study of Cosserat elastic solids and other generalized elastic continua," in: *Continuum Models for Materials with Microstructure*, edited by Muhlhaus, H. B. (Wiley, Chichester).

Lakes, R.S. **(1982)**. "Dynamical study of couple stress effects in human compact bone," J. Biom. Eng. **104**, 6-11.

Lam, D.C.C., Yang, F., Chong, A.C.M., Wang, J., and Tong, P. **(2003)**. "Experiments and theory in strain gradient elasticity," J. Mech. Phys. Solids **51**, 1477–1508.

Midya, G.K. **(2004)**. "On Love-type surface waves in homogeneous micropolar elastic media," Int. J. Eng. Science **42**, 1275-1288.

Mindlin RD **(1964)**. "Micro-structure in linear elasticity," Arch. Rat. Mech. Anal. **16**, 51-78.

Mindlin, RD **(1965)**. "Second gradient of strain and surface-tension in linear elasticity," Int. J. Sol. Struct. **1**, 417–438.

Moilanen, P. **(2008)**. "Ultrasonic Guided Waves in Bone," IEEE Trans. Ultrason. Ferroelect. Freq. Control **55**(6), 1277-1286.

Nicholson, P. H. F., Moilanen, P., Karkkainen, T., Timonen, J., and Cheng, S. **(2002)**. "Guided ultrasonic waves in long bones: modeling, experiment and in vivo application," Physiol. Meas **23**, 755–768.

Njeh, C.F., Hans, D., Wu, C., Kantorovich, E., Sister, M., Fuerst, T., and Genant, H.K., **(1999).** "An in vitro investigation of the dependence on sample thickness of the speed of sound along the specimen," Med. Eng. & Phys. **21**, 651–659.

Ottosen, N.S., Ristinmaa, M., and Ljung, C. **(2000)**. "Rayleigh waves obtained by the indeterminate couple-stress theory," Eur. J. Mech. A/Solids **19**, 929-947.

Papargyri-Beskou, S., and Beskos, D. E. (**2008**). "Static, stability and dynamic analysis of gradient elastic flexural Kirchhoff plates," Arch. Appl. Mech. **78**, 625–635.

Papargyri-Beskou, S., Polyzos, D., and Beskos, D.E. **(2008)**. "Wave dispersion in gradient elastic solids and structures," Int. J. Solids Struct. (*submitted*).

Park, H.C., and Lakes, R.S. **(1986)**. "Cosserat micromechanics of human bone: strain redistribution by a hydration sensitive constituent," J. Biomech. **19**(5), 385–397.

Protopappas, V. C., Baga, D., Fotiadis, D. I., Likas, A., Papachristos, A. A., and Malizos, K. N. **(2005)**. "An ultrasound wearable system for the monitoring and acceleration of fracture healing in long bones," IEEE Trans. Biomed. Eng. **52**(9), 1597–1608.

Protopappas, V. C., Fotiadis, D. I., and Malizos, K. N. **(2006)**. "Guided ultrasound wave propagation in intact and healing long bones," Ultrasound Med. Biol. **32**(5), 693–708.

Protopappas, V. C., Kourtis, I. C., Kourtis, L. K., Malizos, K. N., Massalas, C.V., and Fotiadis, D.I., **(2007)**. "Three-dimensional finite element modeling of guided ultrasound wave propagation in intact and healing long bones," J. Acoust. Soc. Am. **121**(6), 3907-3921.

Protopappas, V. C., Vavva, M. G., Fotiadis, D. I., and Malizos, K. N. **(2008)**. "Ultrasonic monitoring of bone fracture healing," IEEE Trans. Ultr. Ferroel. Freq. Cont. **55**(6), 1243-1255.

Rho, J.Y. (**1998**). "Mechanical properties and the hierarchical structure of bone," Med. Eng. Physics **20**(2), 92-102.

Rose, J.L. (**1999**). *Ultrasonic waves in solid media* (Cambridge University Press, Cambridge).

Ru C.Q. and Aifantis E.C. **(1993)**. "A simple approach to solve boundary value problems in gradient elasticity," Acta Mechanica **101**, 59-68.

Sluys, L.J., de Brost, R., Mulhlaus, H.-B., **(1993)**. "Wave propagation, localization and dispersion in gradient dependent medium," Int. J. Solids Struct. **30**(9), 1153-1171.

Stamoulis, K., and Giannakopoulos, A.E., **(2008)**. "Size effects on strength, toughness and fatigue crack growth of gradient elastic solids," Int. J. Solids Struct. *(in press)*.

Stavropoulou, M., Exadaktylos, G., Papamichos, E., Larsen, I., and Ringstad, C. **(2003)**. "Rayleigh wave propagation in intact and damaged geomaterials," Int. J. Rock Mech. Min. Science **40**, 377-387.

Suiker, A.S.J., Metrikine, A.V., de Borst, R. **(2001)**. "Comparison of wave propagation characteristics of the Cosserat continuum model and corresponding discrete lattice models," Int. J. Sol. Str. **38**, 1563-1583.

Tiersten, H.F., and Bleustein, J.L. **(1974)**. “Generalized elastic continua,” in: *R.D. Mindlin and Applied Mechanics*, edited by Herman, G., (Pergamon Press).

Tomar, S.K., and Gogna, M.L. **(1995)**. “Reflection and refraction of longitudinal waves at an interface between two micropolar elastic media in welded contact,” J. Acoust. Soc. Am. **97**, 822-830.

Tsepoura, K.G, Papargyri-Beskou, S., and Polyzos, D. **(2002)**. “A boundary element method for solving 3D static gradient elastic problems with surface energy,” Comp. Mech. **29**, 361-381.

Vardoulakis, I., and Sulem, J. **(1995)**. *Bifurcation Analysis in Geomechanics* (Blackie/Chapman and Hall, London).

Vardoulakis, I., and Georgiadis, H.G. **(1997)**. “SH surface waves in a homogeneous gradient elastic half-space with surface energy,” J. Elasticity **47**, 147-165.

Wear, K.A., **(2007)**. “Group velocity, phase velocity, and dispersion in human calcaneus in vivo”, J. Acoust. Soc. Am. **121**(4), 2431-2437.

Yang, J.F.C., and Lakes, R.S. **(1981)**. “Transient study of couple stress effects in compact bone: Torsion,” J. Biomech. Eng. **103**(4), 275–279.

Yang, J.F.C., and Lakes, R.S. **(1982)**. “Experimental study of micropolar and couple stress elasticity in compact bone in bending,” J. Biomech. **15**(2), 91–98.

Yerofeyev, V.I., and Sheshenina, O.A. **(2005)**. “Waves in a gradient-elastic medium with surface energy,” J. Appl. Math. Mech. **69**, 61-74.

Yim, H., and Sohn, Y. **(2000)**. “Numerical simulation and visualization of elastic waves using mass-spring lattice model,” IEEE Trans. Ultrason., Ferroel. Freq. Cont. **47**, 550-558.

Yoon, H., Lawrence, J. **(1983)**. “Is bone a Cosserat solid?” J. Mater. Science **18**(5), 1297-1305.

TABLE I: Values of g and h for each one of the six subcases.

Cases	Gradient coefficient g (m)	Intrinsic characteristic length h (m)
Case-1a	5×10^{-4}	10^{-4}
Case-1b	10^{-5}	10^{-4}
Case-1c	10^{-4}	10^{-4}
Case-2a	10^{-4}	10^{-5}
Case-2b	5×10^{-6}	10^{-5}
Case-2c	10^{-5}	10^{-5}

FIGURE CAPTIONS

FIG. 1. (color online) Dispersion curves of the group velocity versus frequency for elastic medium with microstructure.

FIG. 2. (color online) Group velocity dispersion curves of the symmetric modes for a free bone-mimicking plate for the case of the classical (dashed lines) and the gradient theory of elasticity (solid lines) for (a) Case-1a: $g > h$ ($g = 5\times10^{-4}$, $h = 10^{-4}$), (b) Case- 1b: $g < h$ ($g = 10^{-5}$, $h = 10^{-4}$) and (c) Case- 1c: $g = h$ ($g = 10^{-4}$, $h = 10^{-4}$).

FIG. 3. (color online) Group velocity dispersion curves of the antisymmetric modes for a free bone-mimicking plate for the case of the classical (dashed lines) and the gradient theory of elasticity (solid lines) for (a) Case-1a: $g > h$ ($g = 5\times10^{-4}$, $h = 10^{-4}$), (b) Case- 1b: $g < h$ ($g = 10^{-5}$, $h = 10^{-4}$) and (c) Case- 1c: $g = h$ ($g = 10^{-4}$, $h = 10^{-4}$).

FIG. 4. (color online) Group velocity dispersion curves of the symmetric modes for a free bone-mimicking plate for the case of the classical (dashed lines) and the gradient theory of elasticity (solid lines) for (a) Case-2a: $g > h$ ($g = 10^{-4}$, $h = 10^{-5}$), (b) Case- 2b: $g < h$ ($g = 5\times10^{-6}$, $h = 10^{-5}$) and (c) Case- 2c: $g = h$ ($g = 10^{-5}$, $h = 10^{-5}$).

FIG. 5. (color online) Group velocity dispersion curves of the antisymmetric modes for a free bone-mimicking plate for the case of the classical (dashed lines) and the gradient theory of elasticity (solid lines) for (a) Case-2a: $g > h$ ($g = 10^{-4}$, $h = 10^{-5}$), (b) Case- 2b: $g < h$ ($g = 5\times10^{-6}$, $h = 10^{-5}$) and (c) Case- 2c: $g = h$ ($g = 10^{-5}$, $h = 10^{-5}$).

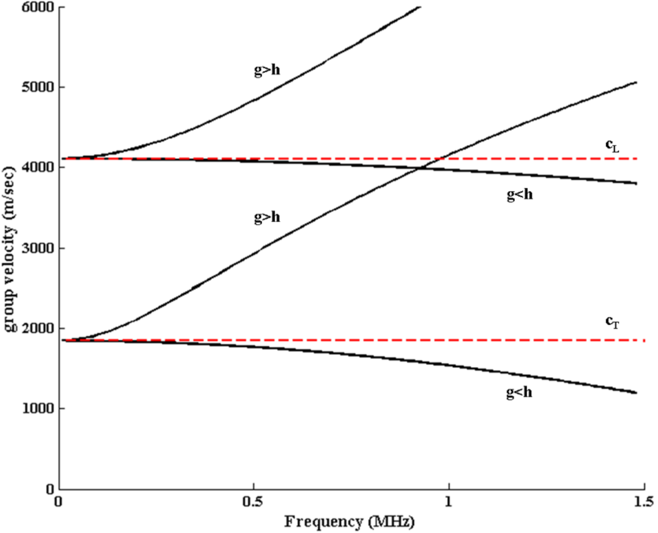

6000
5000
4000
3000
2000
1000
0
group velocity (m/sec)
0
0.5
1
1.5
Frequency (MHz)
g>h
g>h
g<h
g<h
c_L
c_T

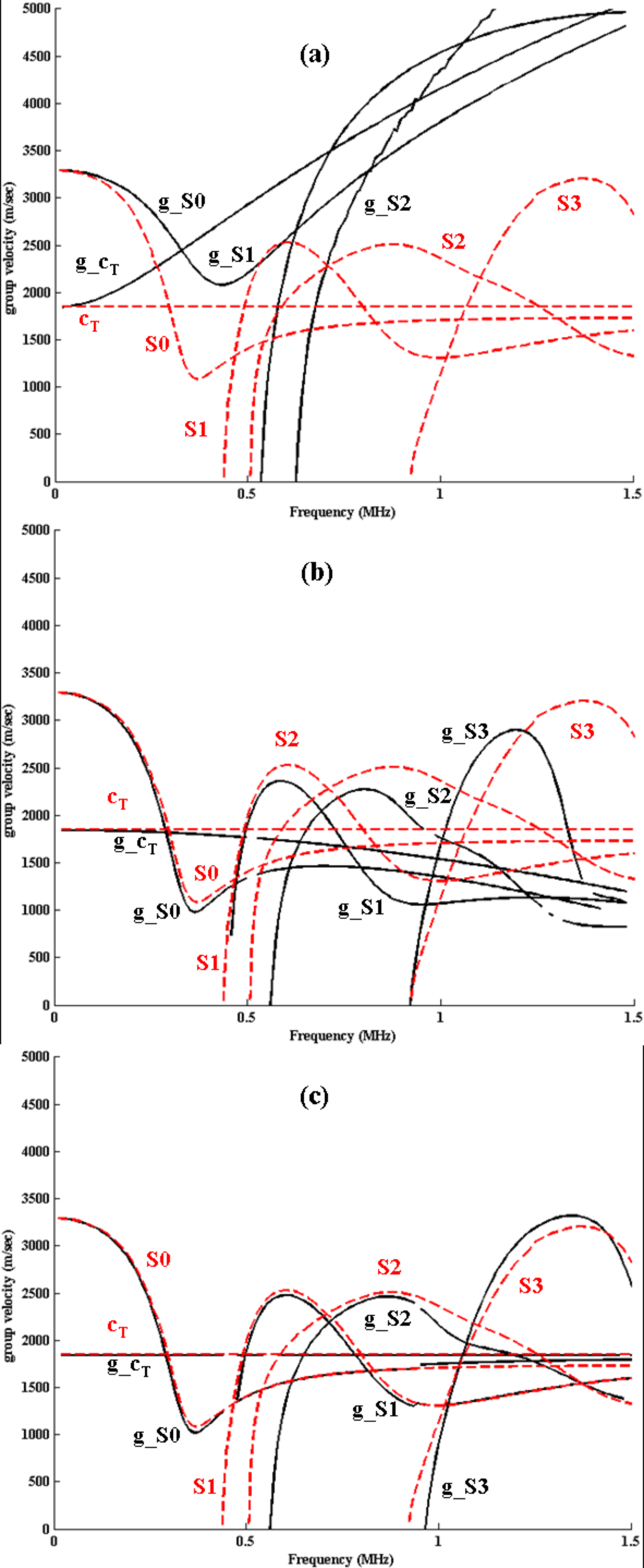

(a)
group velocity (m/sec)
Frequency (MHz)
g_S0
g_S1
g_S2
g_cT
cT
S0
S1
S2
S3
(b)
group velocity (m/sec)
Frequency (MHz)
S2
S3
g_S3
cT
g_cT
g_S2
S0
g_S0
g_S1
S1
(c)
group velocity (m/sec)
Frequency (MHz)
S0
S2
S3
cT
g_S2
g_cT
g_S1
g_S0
S1
g_S3

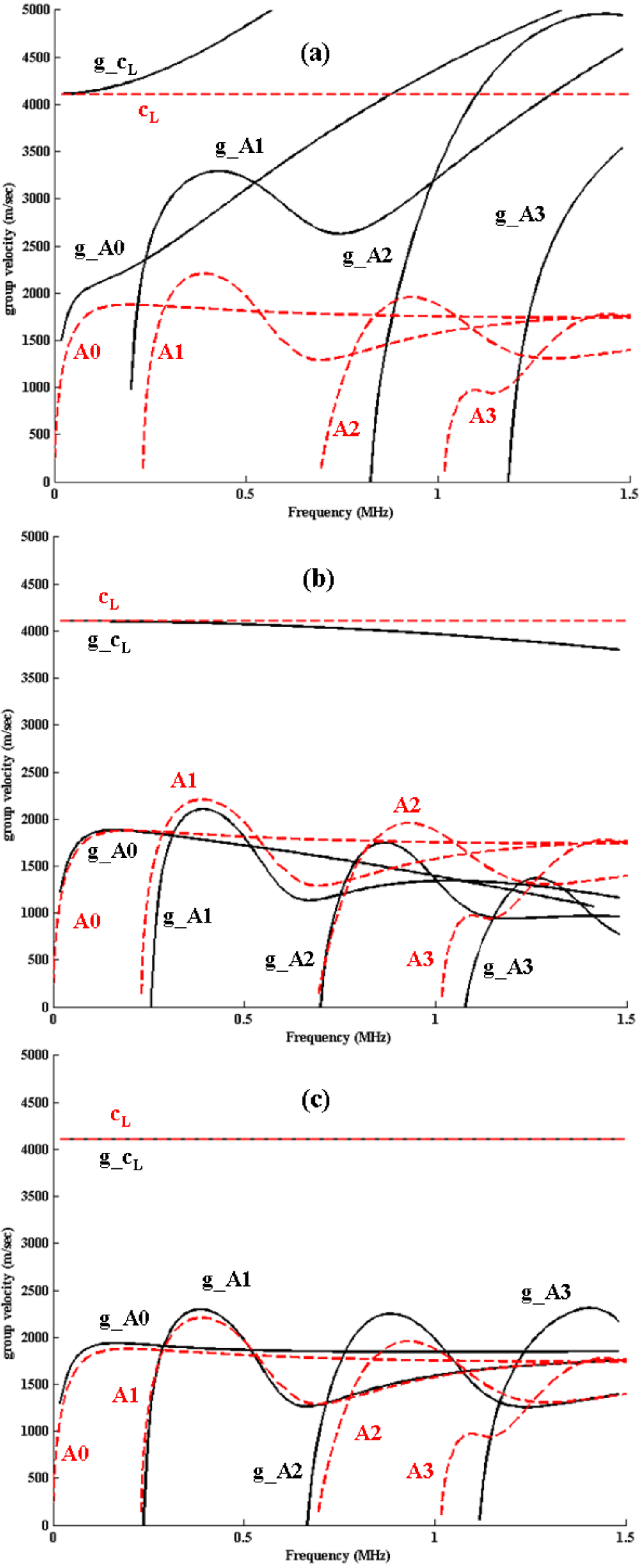
(a)
g_c_L
c_L
g_A1
g_A0
g_A2
g_A3
A0
A1
A2
A3
group velocity (m/sec)
Frequency (MHz)
(b)
c_L
g_c_L
A1
A2
g_A0
A0
g_A1
g_A2
A3
g_A3
group velocity (m/sec)
Frequency (MHz)
(c)
c_L
g_c_L
g_A1
g_A3
g_A0
A1
A0
A2
g_A2
A3
group velocity (m/sec)
Frequency (MHz)

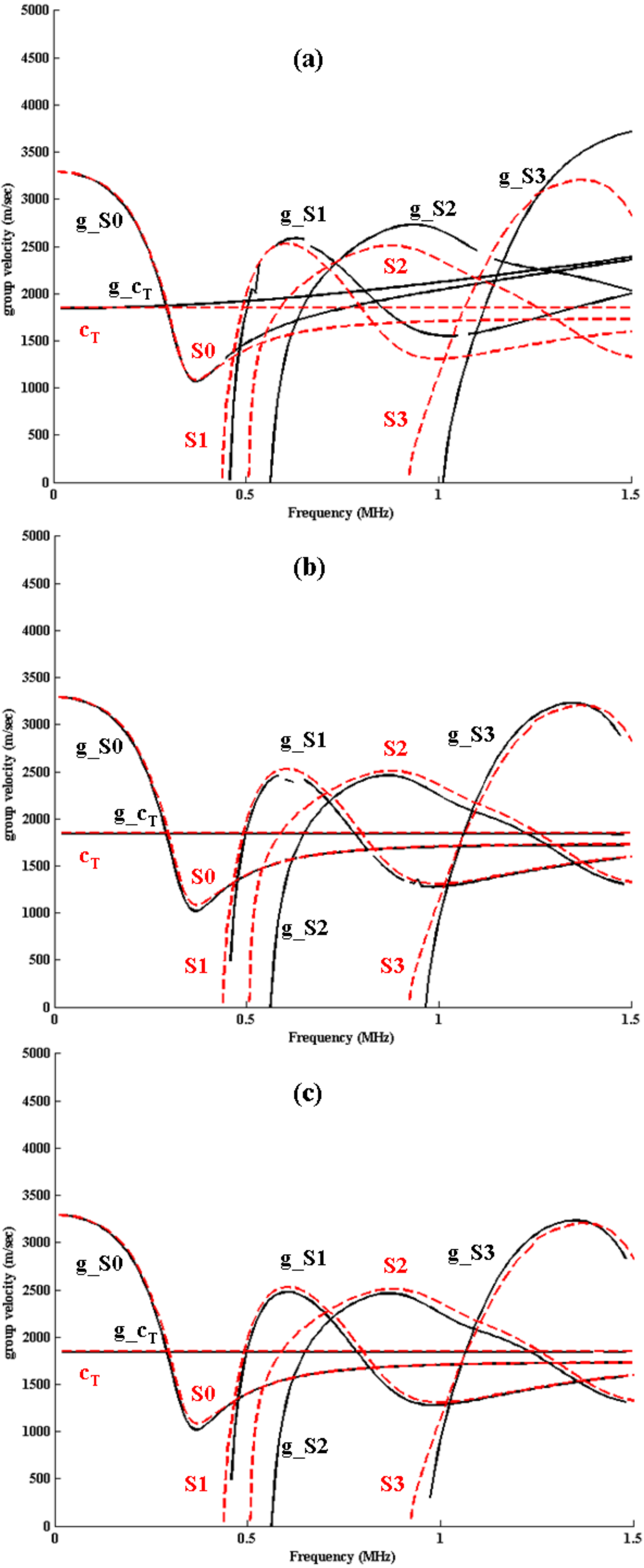
(a)
g_S0
g_S1
g_S2
g_S3
g_c_T
c_T
S0
S1
S2
S3
group velocity (m/sec)
Frequency (MHz)
(b)
g_S0
g_S1
g_S2
g_S3
g_c_T
c_T
S0
S1
S2
S3
group velocity (m/sec)
Frequency (MHz)
(c)
g_S0
g_S1
g_S2
g_S3
g_c_T
c_T
S0
S1
S2
S3
group velocity (m/sec)
Frequency (MHz)

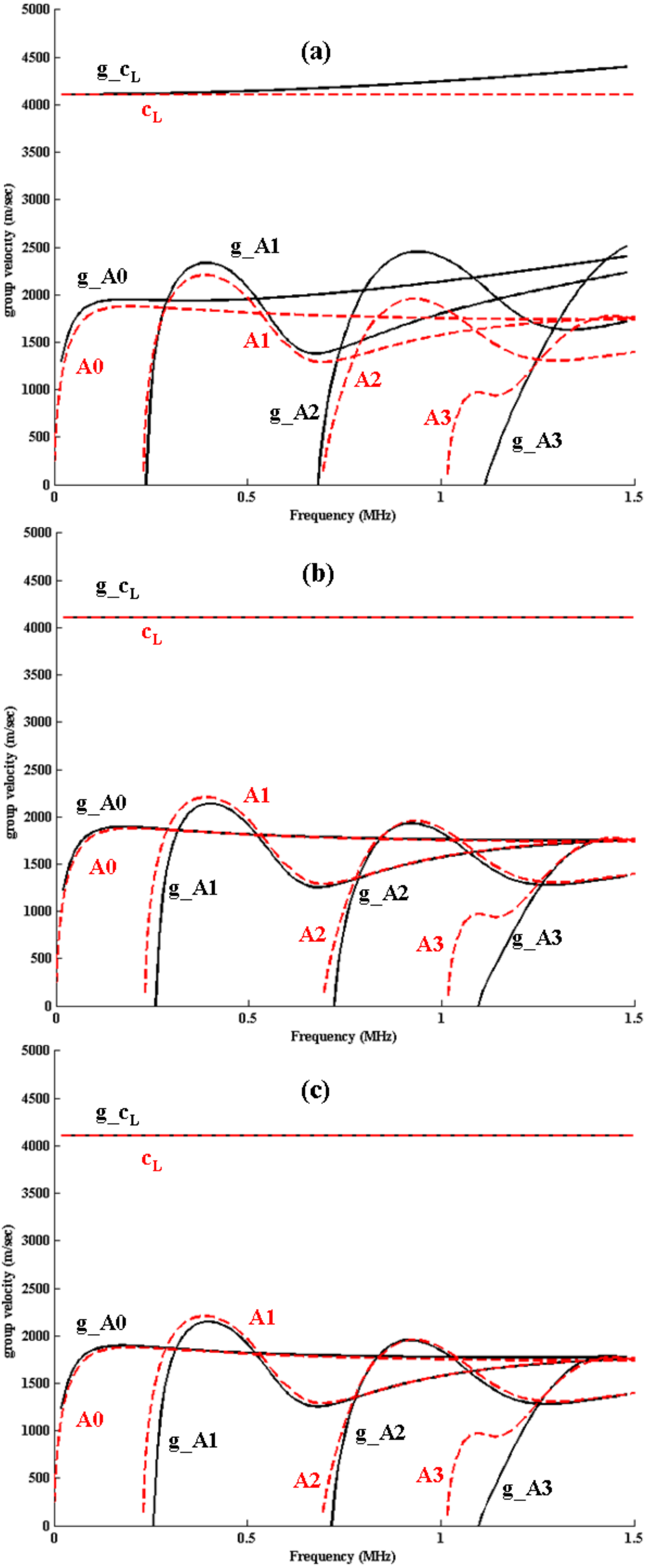
(a)
g_cL
cL
g_A0
g_A1
A1
A0
A2
g_A2
A3
g_A3
group velocity (m/sec)
Frequency (MHz)
(b)
g_cL
cL
g_A0
A1
A0
g_A1
g_A2
A2
A3
g_A3
group velocity (m/sec)
Frequency (MHz)
(c)
g_cL
cL
g_A0
A1
A0
g_A1
g_A2
A2
A3
g_A3
group velocity (m/sec)
Frequency (MHz)